ZANCO Journal of Pure and Applied Sciences

TYPE Original Research
DOI http://dx.doi.org/10.21271/ZJPAS.36.4.8

OPEN ACCESS

*Corresponding author

Bakhtyar Ahmed Mala
bakhtyar.mala@su.edu.krd

RECEIVED :20 /04 2024
ACCEPTED :18/07/ 2024
PUBLISHED :31 / 08 / 2024

KEYWORDS:
TLS,
Point clouds accuracy,
Different Materials surface and colors,
scan Angle and range,
and Reflectivity of materials.

The impact of object properties and scan geometry on the quality of TLS data

Bakhtyar Ahmed Mala[1*], Dleen Muhammed Salih Al-shrafany[1]

[1]Department of Geomatics (Surveying) Engineering, College of Engineering, Erbil, Salahaddin University-Erbil, Erbil ,Kurdistan Region, Iraq

ABSTRACT

Object surface Properties, range, and measuring trip time are main variables affecting the positional accuracy of the computed point clouds by the terrestrial Laser Scanner (TLS). In this research, Practical experiments were carried out by Faro focus premium TLS in order to investigate how does the variation of surface roughness and its reflectivity affect the positional accuracy of the measured scanner data at different scan angles and ranges. For this purpose, different materials that have distinct surface properties were conducted (glass, steel, wood, ekoplast, and total station (TS) sheet targets). Also, to examine the impact of the surface color, three of those selected materials have been painted with RGB color and black and white colors as well. About 54 scans were recorded during the experiment as all materials were scanned at three different scanning angles of (0˚, 30˚, and 60˚) and at ranges of 5 and 20 meters. The experiment's findings reveals that, at various incident angles, smooth surfaces have a greater impact on the accuracy of the scanned objects to create 3D point clouds than do rough surfaces. Furthermore, the total RMSEs in the point clouds position that measured from surface painted with red and black colors is greeter and higher than those measured from blue, green, and white colors painted surfaces. Interestingly, the total station target had never reflects the laser beam at all incident angles and ranges for class-1 laser beams. Additionally, the intensity of various materials varies. For example, the smooth materials steel and glass have varying degrees of accuracy because of their respective characteristics of the surface.

1. Introduction

Laser scanner systems used two-direction travel peroids Time of Flight (TOF) for calculating the range (ρ) between the scanned objects and the scanner. As there is no need to put any target on the surface of the scanned materials, reflector-less TLS systems are typically applied in the object scanning process. Therefore, the range is dependent on how much of the object's sufficient returned signal reaches the scanner's photo-detector. The properties of the materials affected on the signal reaches the scanner range detector.

There are numerous approaches, ranging from the conventional way to the contemporary methods, to produce an accurate 3D surfance of the objects. Using a camera, satellite sensors and scanners, image-based and laser-based techniques are the most popular and recent methods (Chan et al., 2015a). The most modern and precise method is Terrestrial Lasre Scanning (TLS) that used in this field.

It's important to note that a diverse types of parameters, including measurement geometry, material qualities, weather conditions, and instrument effects, all had an impact on the computed point clouds (S Soudarissanane, 2016). Some of the scanners' properties were included their high measurement data, accuracy of reflector-less natural scanning technology and high spatial density data. The TLS geometry for scanning (Tan et al., 2018), the error in oscillating scanner mirror (Bae & Lichti, 2007), divergence of the beam (Sylvie Soudarissanane et al., 2009), scan angle (Sylvie Soudarissanane et al., 2008), the calibration instrument process of the scanner (Chan et al., 2015b) and (Abbass et al., 2023), and the manufacturing company for instrument types such as (Faro, Topcon, Leica, and Trimble) all had an influence on the accuracy of measured point clouds.

However, one of the main variables influencing the quality of the observed point clouds, along with incidence angle and distance, is scanning geometry (Lichti & Harvey, 2002), (Amer et al., 2018), (Sylvie Soudarissanane & Ree, 2007). Furthermore, there were many other problems during the data processing in terms of software obstactions, performing target methods, registration and georefrecessing data (Murtiyoso & Grussenmeyer, 2018), (Bae & Belton, 2012), (Abdurrahman Farsat1* et al., 2014), (Date et al., 2019), (Abbas et al., 2014), and (Steinvall, 2007). Different surface materials with different scan angles scanned for various purposes, including deformation monitoring of the manmade objects (Gordon et al., 2000), structure of the bridge monitoring (Gordon et al., 2000), building facade measurements (Balzani, n.d.) and (Mala et al., 2016) were used TLS to document and apply some of the materials. Evidently, the impacts of color, surface property, and material type vary in tems of accuracy during scanning these kinds of objects (Kostrikov et al., 2020), (Huang et al., 2023), and (Huang et al., 2023).

This study is focused on performing different scans for different types of materials taking into consideration the variation in two main parameters: Firstly: surface roughness variation, secondly: Surface color variation. All this under identical weather condition. As this paper aims to investigate the impact of the object (materials types) properties and scanning geometry on the quality of TLS point clouds data in terms of precision and positional accuracy.

2. Materials and Methodology

2.1 Materials

Regardless of whether the material is constructed of natural or artificial materials, surface roughness and reflectivity are two important characteristics parameters that could have a substantial impact on the precision and quality of the scanned point cloud data (Lichti & Harvey, 2002).

Three individual surfaces were painted in (RGB and black and white) colors, and four different materials were prepared for scanning as part of this research technique. Two main factors were the criteria basis for material’s selection in this research selection : First, the most useful/common used material found in structures constructed by humans, like buildings. Second, a noticeable difference occurance in the surface roughness and reflectivity of the material. Hence Glass, steel, wood, and Ekoplast were the materials used for examining the effect of material type on scanning quality, while Astropol, gypsumboard, and Alicobon were the painted materials that used for examinning the effect of color variation on scanning quality. Each of these materials has a notable variance in surface roughness and is primarily utilized in man-made constructions.

Before the scanning process began, the characteristics of each aforementioned material were examined, including the sample's dimensions, which are as follows: Glass with a thickness of 6 mm and dimensions of 80 cm by 80 cm is used as mackle for reflecting the laser signal to the scanner and avoid noises. Steel, sample is about 80 cm by 80 cm in size and 1.8 mm thick (Figure 1).

Regarding to wood material that is primarily employed in the construction of bookcases, lockers, doors, and structures. Its sample has the same dimensions (80 cm by 80 cm) and a thickness of only 8 mm. Last but not least, Ekoplast, a substance that is typically used to plaster a building's façade in an effort to separate and release sound, heat, and cold. This type of substance must be combined with water to create products like gypsum, stucco, and parget. An Ekoplast sample measuring 20 mm in thickness and 80 cm by 80 cm in size has been created for this study. See Figure 1

Alicobon is one of the materials that is most frequently used in construction, such as for building decoration and tableau writing. Therefore, in order to reflect the laser beam's signal, the material's reflectivity and roughness must be taken into account based on the colors used. This material dimension is 80 cm by 80 cm and is only 18 mm thick. Each of the 25 squares that made up the initial face (as it can be seen from Figure 1), measured 16 by 16 centimeters. All five colors were used in each row and column. The other face was painted in four different colors, and each square was 40 by 40 centimeters.

Gypsum board is another common material for plastering interior walls of buildings. Therefore, based on the colors, the material's reflectivity and roughness properties must be taken into account. The material's roughness is determined by measuring the diameter of the laser beam footprint. Its dimension is 80 cm by 80 cm and it is only 10 mm thickness. Green and red paint were used to paint the first face, Figure 1, which was divided into two (40 by 80) cm parts. The other side was painted the same size as the first face in blue and red.

Astropol isAnother substance frequently used for plastering outside walls of buildings. Therefore, it is necessary to take into account the material's reflectivity and roughness. Bidirectional Reflectance Distribution Function (BRDF) and laser beam diameter allow materials to be classified as rough in terms of roughness. It is 80 cm by 80 cm dimension and is 50 mm thickness. Figure 1 shows a single face painted in black and white that is separated into two rectangles, each measuring (40 by 80) cm. Figure 1 displays all the prepared samples of materials that has been used in this study while Table 1 summarize the dimensions and relevant characteristics of all those materials that conducted to achieve the purpose of this research.

Table 1: Summery of the selected materials for scanning in different scan angles and ranges.

No.	Materials	Size	Thickness (mm)	Roughness	Painting
1	Glass	80 cm x 80cm	6	Smooth	Not painted
2	Steel	80 cm x 80cm	1.8	Smooth	Not painted
3	Wood	80 cm x 80cm	8	Rough	Not painted
4	Ekoplast	80 cm x 80cm	20	Rough	Not painted
5	Astropol	80 cm x 80cm	50	Rough	Painted
6	Gypsum board	80 cm x 80cm	10	Rough	Painted
7	Alicibon	80 cm x 80cm	18	Smooth	Painted
8	TS targest	4 cm x 4 cm	1	smooth	Not painted

However, based on the BRDF and the scanner beam foot print area, the materials glass, steel, and alicobon are regarded as smooth surfaces, but the materials wood, ekoplast, gypsumboard, and astropol are considered as rough surfaces based on the following equation (1). BRDF is a method the gives the ratio between incoming and outgoing radiance.

$$BRDF\left(i,\alpha_i,r,\alpha_r,\lambda\right)=\frac{L(i,\alpha_i,r,\alpha_r,\lambda)}{E(i,\alpha_i,\lambda)} \qquad (1)$$

In order to investigate the impact of smooth and highly reflecting surfaces on the accuracy and quality of observed point cloud data at varying incident angles, five TS targets were fixed on the prepared sample of each material. TS target is a 4 × 4 cm Adhesive sheet target, and it has a thickness of only 1 mm or less. These targets have the maximum amount of reflectivity and are perfectly smooth.

Figure 1: All materials performed for different angles of scanning and ranges using faro focus premium instruments, materials from left to right first row are: Glass, Steel, Wood, and Ekoplast, and second row are: painted materials from smooth to rough materials Alicobon, Gypsumboard, and Asropol

2.2 Methodology

The approach of this study was carried out in three steps: The first step is choose and prepare material samples that satisfy the necessary dimensions and requirements, in order to comply with the specifications for an accurate scanning technique. Also in this step a necessary mechanical stand to hold the material samples correctly and vertically has been manufactured in order to simulate the actual situation. The second stage involves configuring the TLS and establishing the distance between the material stand and the scanning station. Lastly, carry out the procedure of scanning the material sample at different scanning angles as a third step. The technique flowchart used to accomplish the goals of this research is shown in Figure 2.

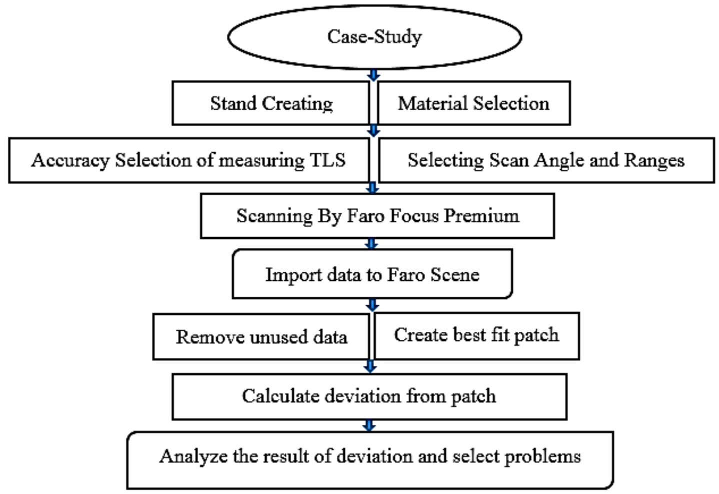

Figure 2: Flowchart illustrates the procedure of scanning and analyzing data

It is important to note that the creation of a wooden stand is essential for achieving accurate and high-quality material sample scanning and simulating the real situation as much as its possible. This is because the range between the material sample and the scanner instrument must be fixed as an observed target, the scanning angle must be controlled, and the material sample must remain vertical throughout the scanning process. Wood was used to make this platform because it was inexpensive and lightweight, making it easy to move from one location to another. It is component from two distinct parts in terms of design and structure: The first component (top part), a frame with dimensions of 1 x 0.8 m, which is utilized to place and secure the material tests inside of it. importantly, this frame is made to be as a detachable component from the object body of the construction, making it simple and quick to remove or alter and then reattach a sample of a different material. The second component (Lower part) is circular stand constructed from wood. This component is 50 centimeters above the ground. This component of the construction has two bases in circular manner to control the verticality, top and down. At the circular base centers have two central small wholes that lie on a single vertical direction, as it can be seen in

Figure 3. The Topcon (GTS-230N) total station instrument's centering laser beam was utilized to regulate this verticality. Additionally, a small sharp nail added next to the upper circular edge portion in order to change and controlling the scanning angles.

Figure 3: Verify the verticality of the stand by using the centering vertical laser beam of the total station equipment. The verticality test is shown by the two images on the right, while the controlling scan angle is shown in the left image.

2.3 Scanning Materials

All material samples were scanned at three scan angles: (0˚, 30˚, and 60˚), with two different range between the scanner and the material's stand approximately 5m and 20m. Six scans were taken per material using Faro focus premium laser scanner instrument. Figure 4 illustrate the principal of scanning objects.

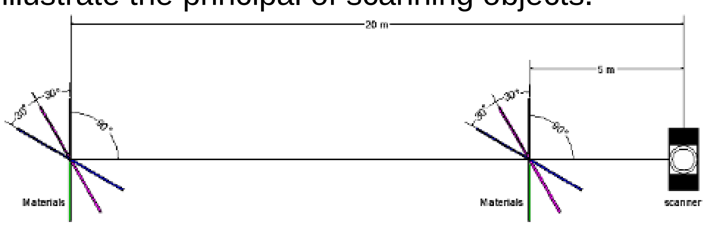

Figure 4: principal of Scanning materials using Faro focus premium TLS in 5m and 20m range and three different incident angles.

Figure 5 below illustrate some samples of scanned data for all aforementioned materials at 5m range and zero degree incident angle. figures in first row (a,b,c and d) are arranged according to their surface's roughness degree from smooth to rough respectively as follows: glass, steel, wood, and ekoplast. While figures in second row (e,f,g and h) represents the painted materials from left to right also arranged from smooth to rough surfaces (e, f : alicobin, g: gypsumboard, and h: astropol).

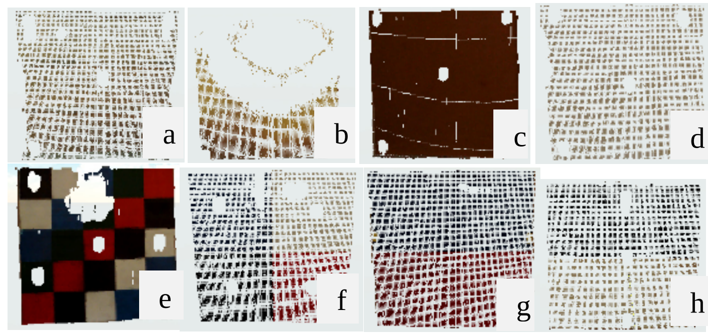

Figure 5: From left to right first row: (a) glass, (b) steel, (c) wood, and (d) ekoplast scanned materials and second row (e, f) five and four colors on smooth Alicobon surface, and (g, h) are two by two colors on rough gypsumboard and astropol surface respectively. All scans taken at 0˚ and 5m range.

As stated in Table 2 below, the Faro focus premium TLS equipment were utilized for the scanning process. In addition, Faro scene particular software were applied for analyzing the collected scanned point clouds because it is a specific software that used with the faro scanners.

Table 2: Faro focus premium laser scanner specifications

Names	Specifications of faro focus premium
Instrument name	Faro Focus Premium350 A
Field of view	V. and H angles ae 300˚ and 360˚, respectively
one Scanning windoow	From -60˚ to 90˚
Laser class	Laser class 1
Beam divergance	0.3mrad (1/e)
Beam diameter	2.12mm (1/e)
weight	4.2 kg
Scanning model	Pulse-based method
Accuracy of single measurement	Position 1mm @ 10m and 19 arcsec. For angle
Range	0.5m to 350 m
Operation temperature	5˚ C to +40˚ C
Dimensions	230 x 183 x 103mm
Data storage	Internal SDHC, SDXC, 32GB cart

In addition to the already scanned materials separately, five (4cm x4cm) adhesive TS targets were carefully placed near to the corners and in the center of scanned material sample surface in order to examine the effects of highly smooth and reflective surfaces on the accuracy and quality of measured scanned data at different angles of scanning objects.

As well as to examine the deviations and finding the noises in the measurements, a best fitted patch were created to cover the whole data followed by calculating the shortest distance from the patch surface to the measured point cloud on every single surface, then the summation of the square root for that distance were measured to find the overall RMSEs of the scanned data based on the selected point clouds.

3. Results and Discussion

3.1 Effects of Rough surface

In the Practical experiments, two different group of rough surfaces were scanned, the first group measured materials were scanned with the original material (wood and ekoplast), followed by the second group material (Astropol) were painted in different colors.

3.1.1 Rough Surface Original Samples

It is important to note that temperature, roughness, and certain material qualities are shown to affect the number of reflected point clouds. For example, when the scan angle increases, the quantity of reflected point clouds from rough surface materials gradually decreases. this is happened due to the micro-facet objects on the surface of the rough objects. Figure 6 shows the rough surface objects (wood and ekoplast) that scanned in three different incident angles.(0˚, 30˚, and 60˚).

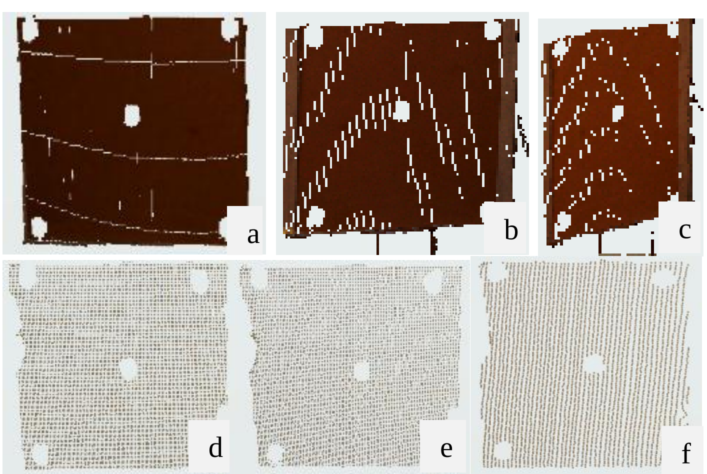

Figure 6: Scanned Rough surface materials (wood and Ekoplast) at 5m range. a: wood at 0˚, b: wood at 30˚, and c: wood at 60˚. d: Ekoplast at 0˚, e: Ekoplast at 30˚, and f: Ekoplast at 60˚.

When the best fitted patch were create for the scanned data, the shortest distance for randomly selecting 15 point clouds to the patch surface were measured (in order to find out their deviation from the best fitted patch) at all three different incident angles (0˚, 30˚, and 60˚), the square of these deviations calculated. Then, the Root Mean Square Errors (RMSEs) for each materials were found based on the following equation (2).

$$RMSE = \sqrt{\frac{\sum_{i=1}^{n}\left(x_i - x^{'}\right)^2}{n}} \qquad (2)$$

Where: $(x_i - x^{'})$ is the measured deviation from the best fitted patch.

The overall RMSEs of wood and ekoplast will decreases with increasing the scan angle due to the micro-facet objects on the surface of the rough objects. In other hand, the RMSE of the wood is greater than the ekoplast due to having the micro-facet parts on the surface of the ekoplast higher than the wood surface material. Table 3 below shows the deviation from the best fitted patch for rough wood and ekoplast surface materials in three different scan angles (0˚, 30˚, and 60˚), and represents the overall RMSE for the selected 15 point clouds at all three scan angles. The maximum RMSE appeared in 0˚ wood material that is 2.4mm, while the minimum RMSE occurred at 60˚ ekoplast material with 1.3mm. All of the deviation were calculated only for 20m distance range to easy understanding to the reader.

Table 3: Deviation from the best fitted patch for wood and ekoplast at 20m range in three different scan angles.

Points	Wood 20m (mm)			Ekoplast 20m (mm)		
	0d	30d	60d	0d	30d	60d
1	2	3	1	1	0	1
2	2	2	0	2	2	1
3	1	2	2	2	2	2

4	3	1	1	1	2	2
5	3	3	2	3	1	1
6	1	0	0	2	2	1
7	0	1	1	2	1	0
8	2	2	2	0	0	1
9	1	1	1	1	2	1
10	3	3	0	3	1	2
11	4	0	1	0	2	1
12	2	1	2	2	1	1
13	3	3	2	1	0	1
14	2	0	1	3	2	2
15	3	1	2	1	0	1
RMSE	2.4	1.9	1.4	1.9	1.5	1.3

3.1.2 Rough surface coloured material

On the other hand, when the rough surface material is colored , the intensity and reflectivity was different from a color to another. Which in turn shown its effectness on the reflected point cloud numbers and the amount of energy power for every the single reflected point cloud. For instance, the returned number of point cloud data from rough white surface material was gently decreases with increasing incident angle, while decreasing point clouds are different on the same material were covered by black color. this is happened due to the micro-facet objects on the surface of the rough surfaces where reduce the effect of the incident angle and color intensity. Figure 7 shows the rough surface objects that scanned in three differentt incident angles.

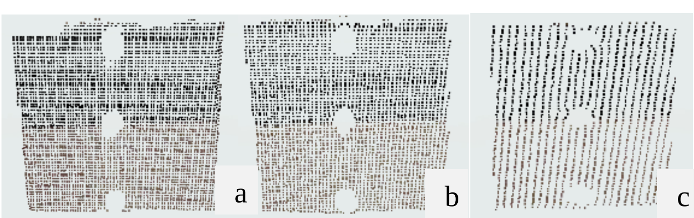

Figure 7: Black and white colors on the rough astropol surface material at 20m range. a: 0˚, b: 30˚, and c: 60˚ scan angles.

Similarly, best fitted patch surface created for the reflected point clouds. The deviation and overall RMSEs were calculated as well based on the selecting 15 point clouds. Results reveals that the overall RMSE decreases with increasing the scan angle due to decreasing the intensity of the returned signals that the scanner cannot recognize the differences between the different colors. As shown at 60˚ incident angle the difference RMSE between black and white colors less than the difference of RMSE at 0˚ between black and white colors. In other hand the RMSE of the black color is greater than the white color due to the difference in intensity between black and white colors. Table 4 below shows the deviation from the best fitted patch for the rough colored Astropol material surface (black and white) colors at three different scan angles, and represents the overall RMSE for the selected 15 point clouds at all three scan angles. The maximum RMSE appeared in 0˚ black color, while the minimum RMSE happened at 60˚ white color.

Table 4: Deviation from the best fitted patch for black and white color on the rough surface (Astropol) at 20m range in three different scan angles.

Points	Black 20m (mm)			White 20m (mm)		
	0d	30d	60d	0d	30d	60d
1	1	1	1	0	2	1
2	2	0	0	1	0	0
3	0	1	1	2	1	0
4	2	0	2	1	1	1
5	2	2	0	1	1	1
6	0	3	1	1	0	0
7	1	1	0	0	1	1
8	2	2	2	1	0	0
9	1	1	1	2	2	2
10	2	0	0	1	1	1
11	3	1	2	1	1	0
12	1	0	1	0	0	1
13	1	1	0	2	1	0
14	0	1	1	1	0	2
15	1	1	0	0	1	1
RMSE	1.5	1.3	1.1	1.2	1.0	1.0

3.2 Effects of Smooth Surface

Two different smooth surfaces were scanned in the same way similar to the rough surface case. The first group measured materials were scanned with the original material (glass and steel), and then the second material were painted in five different colours on the Alicobon smooth surface material. All this at the same configuration of 5m distance range and at 3 different incident angles.

3.2.1 Smooth Original Surface Material

On the scanned smooth surface materials valuable problems were appeared. At the beginning, when the incident angle is closed to zero, the effect of the incident angle no appeared on the point clouds accuracy, but the effect on the Sun shine makes a big noise on the accuracy of the measured point clouds. This noise can be easily seen in the zero degree incident angle of steel materials. In other side, when the incident angle increases more noises appeared in the reflected point clouds from the smooth surface materials due to decreasing the amount of the returned signal of the laser beam to the scanner, Figure 8 shows all of these noises on the smooth surface materials. As first row shows the glass material at (0˚, 30˚, and 60˚) scan angle as (a, b, and c) respectively. While the second row shows steel material with the same incident angles and all of the scanned data measured in 5m distance range.

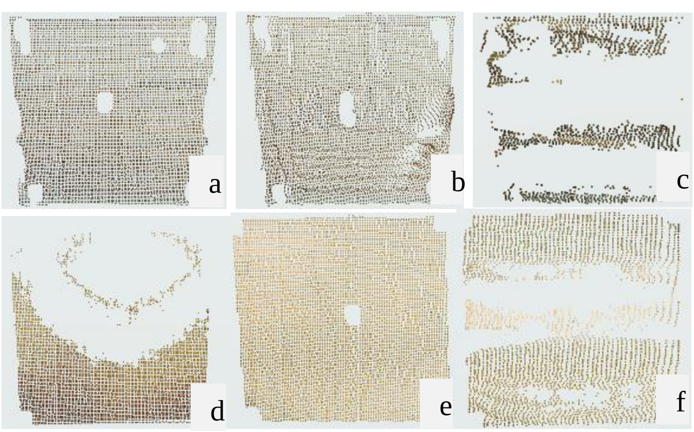

Figure 8: Smooth surface scanned materials glass and steel at 5m range. a: Glass at 0˚, b: Glass at 30˚, and c: Glass at 60˚ scan angles. And d: Steel at 0˚, b: Steel at 30˚, and c: Steel 60˚ incident angles.

The deviation from the best fitted patch and overall RMSEs of the smooth surfaces (glass and steel) materials were calculated based on the selecting 15 point clouds. The overall RMSE increases with increasing the scan angle due to the effect of the Sun rays and changing the intensity of the returned signals the scanner. In other hand, except at 0˚ scan angle the RMSE of the steel is less than the glass due to the difference in intensity of the reflected energy between steel and glass material and penetrate a part of laser beam through the glass material. Table 5 below shows the deviation from the best fitted patch for smooth glass and steel surfaces at three different scan angles, and also the overall RMSE for the selected 15 point clouds at all three (0˚, 30˚, and 60˚) scan angles. The maximum RMSE occurred at 0˚ scan angle for steel about 15.1mm, as well as the minimum RMSE occurred for steel material but at 30˚scan angle about 3.5mm.

Table 5: Deviation from the best fitted patch for glass and steel smooth surface at 20m range in three different scan angles.

Points	Glass-20m (mm)			Steel-20m (mm)		
	0d	30d	60d	0d	30d	60d
1	10	2	6	2	2	3
2	7	11	9	15	2	2
3	3	8	8	19	6	5
4	9	2	9	18	5	3
5	10	12	10	8	1	2
6	4	3	5	2	2	4
7	8	4	4	3	5	6
8	5	5	8	4	4	4
9	6	8	4	6	4	1
10	9	7	5	14	2	7
11	8	4	6	24	3	6
12	4	8	7	18	2	5
13	7	6	7	31	5	5
14	4	5	9	10	2	3
15	5	10	7	15	2	1
RMSE	7.0	7.0	7.2	15.1	3.5	4.2

3.2.2 Smooth surface Coloured material

Similarly, for the scanned smooth surface materials that painted in five different colors these problems appeared that where appeared in the glass and steel smooth surface materials. Firstly, at zero degree incident angle it means scanned data without the effect of the incident angle, where the Sun shine coincide with the direction of the laser beam makes a gap for this area, the number of returned point clouds in this area closed to zero, see Figure 10. This noise can be easily seen at zero degree incident angle of painted material with five colors. On other side, when the incident angle increases also the noises increases on the smooth surface materials due to decreasing the amount of the returned signal of the laser beam and changing the amount of signal to noise ratio. This is clearly appeared on the black colour, because generally the intensity of the black colour is less than the other colour and when the incident angle increases the intensity also decreases. If the returned signal is too weak, it is difficult to detect as a reflected signal. When the intensity magnitude is smaller than the noise level of the detection unit, it indicates the signal is weak. For longer ranges or higher incident angles, the detection of the signal becomes harder, this then produce noises especially on the black colour smooth surface and it has unbelievable data on this surface. Figure 9 shows all of these noises on the smooth coloured surface materials. First row shows the alicobon smooth material at (0˚, 30˚, and 60˚) scan angles from left side to right side with five colours in 5m range, while the second row shows same material with the same incident angles and 20m range that painted by four colours.

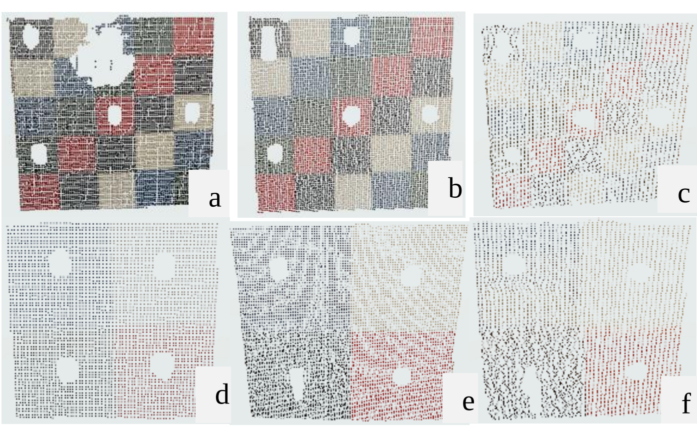

Figure 9: Painted smooth surface alicobon material with two different range and sizes. a: Alicobon at 0˚, b: Alicobon at 30˚, and c: Alicobon at 60˚ scan angles in 5m ranges. And d: Alicobon at 0˚, e: Alicobon at 30˚, and f: Alicobon at 60˚ scan angles in 20m ranges.

The deviation from the best fitted patch and overall RMSEs of RGB, black and white colors on the smooth (Alicobon) surface material were calculated based on the selecting 15 point clouds. The overall RMSE will increases with increasing the scan angle for black and red colors due to decreasing the intensity of the returned signals that the scanner cannot recognize the differences between the different colors and the intensity of the point clouds closed to each other. Table 6 below shows the deviation from the best fitted patch for smooth alicobon material surface for all five selected colors at three different (0˚, 30˚, and 60˚) scan angles, and represents the overall RMSE for the selected 15 point clouds at all three scan angle. The maximum RMSE appeared in 60˚ black color that is 5.9mm, while the minimum RMSE happened at 60˚ white color. The RMSE of black and red colors are greater than the other color due to the difference in the difference in intensity between colors.

Table 6: Deviation From the best fitted patch for RGB, black, and white color on smooth surface (Alicobon) at 20m range in three different scan angles.

Points	Red 20m (mm)			Green 20m (mm)			Blue 20m (mm)			Black 20m (mm)			White 20m (mm)		
	0d	30d	60d	0d	30d	60d	0d	30d	60d	0d	30d	60d	0d	30d	60d
1	6	3	2	3	3	3	1	1	0	3	4	5	2	1	2
2	5	6	4	2	2	3	3	2	1	4	5	4	3	2	1
3	3	4	6	2	3	3	1	2	0	5	6	3	2	0	2
4	1	4	5	1	1	1	4	1	3	5	4	7	1	2	1
5	4	3	6	2	2	0	2	3	2	2	6	6	2	1	1
6	5	6	2	4	2	2	1	1	2	3	5	5	1	1	2
7	5	4	5	2	0	2	2	0	1	6	4	8	2	2	1
8	4	2	4	3	3	0	2	2	0	4	7	6	3	2	1
9	3	5	5	1	2	1	1	3	1	5	4	7	0	1	0
10	2	5	3	2	1	0	3	1	2	3	4	6	1	2	0
RMSE	4.1	4.4	4.4	2.4	2.1	1.9	2.2	1.8	1.6	4.2	5	5.9	1.9	1.6	1.3

3.2.3 Smooth Surface Material Noises During Scanning Materials

According to the practical experiment, obvious noises stats occurred in the measured point clouds from the smooth surface materials in regards to the surface colour, clarity and its reflectivity. The occurrence of these kind of noises actually can be justified according to the following effects: Firstly, the effect of the Sun rays. If the incident angle of the Sun coincide with the laser beam scan angle, so, the signal will not reflected properly to the scanner and will makes a miss locating positions in the position accuracy of the measured point clouds, because the intensity of the laser signal dramatically changed or increased. This changes, depends on the laser class types of the scanner. Secondly, when the incident angle increases and reached to 60˚ or greater than the amount of the returned signal, so it will become insufficient to detect the correct position of the point clouds or it not measure the point clouds at all. This is happened for some case especially when the surface is smoother or the reflectivity of the material is weak. Finally, in a specific case when the surface of the material has a high reflectivity and smoothness, no point clouds returned to the scanner in any incident angle and range, this is true for laser class-1 scanners, while for these scanners have laser class-3 they reflected the laser beam, but it is faster than normal which lead to makes error in the positioning (Mala & Al-shrafany, 2023). For instance, TS targets were placed on the surface of the materials, there is no reflected point clouds on these targets at all incident angles and ranges. Figure 10 shows all of these three errors that happened due to the smoothness of the material surfaces.

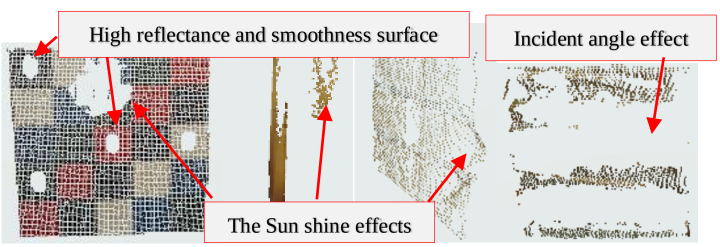

Figure 10: Errors happened on the smooth surface materials due to the Sun shine, incident angle and high reflectivity and smoothness of the materials.

Below Figure 11 shows the deviation of the ten selected point clouds on the surface of the glass and steel materials having noises due to the Sun rays. Left figure shows the deviations for steel material at zero degree scan angle and right figure shows the deviations of the noises from glass material at 30 degree scan angle.

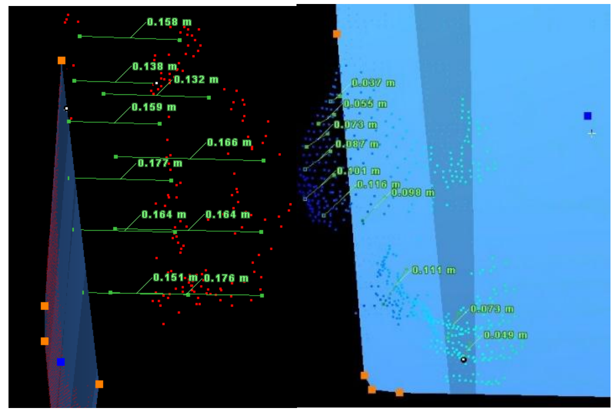

Figure 11: deviation from the best fitted patch for these points have noise during the scanning procedure. a: Steel at 0˚, and b: Glass at 30˚.

Interestingly, one of the most important factors that effect on the smooth surface materials is the Sun rays. When the Sun light coincide with the scan angle effects on the intensity of the reflected signal and produce noise on this position. Table 7 below illustrate the overall RMSEs on glass and steel material's noises due to the Sun shine. The RMSE of the glass at 30˚ incident angle is 68.61mm, and the RMSE of the steel material at zero degree scan angle is 129.91mm. The effect the Sun shine on the steel surface material is greater than on the glass smooth surface as shown in Figure 12 below.

Table 7: Deviation from the fitted patch for these points that have noise due to the Sun shine during scanning objects.

Problems-5m-0d (mm)			Square Root	
Pts.	Steel 0d	Glass 30d	Steel 0d	Glass 30d
1	158	37	24964	1369
2	138	55	19044	3025
3	159	73	25281	5329
4	177	87	31329	7569
5	164	101	26896	10201
6	151	116	22801	13456
7	176	98	30976	9604
8	164	111	26896	12321
9	166	73	27556	5329
10	132	49	17424	2401
		Sum	253167	70604
		RMSE	129.91	68.61

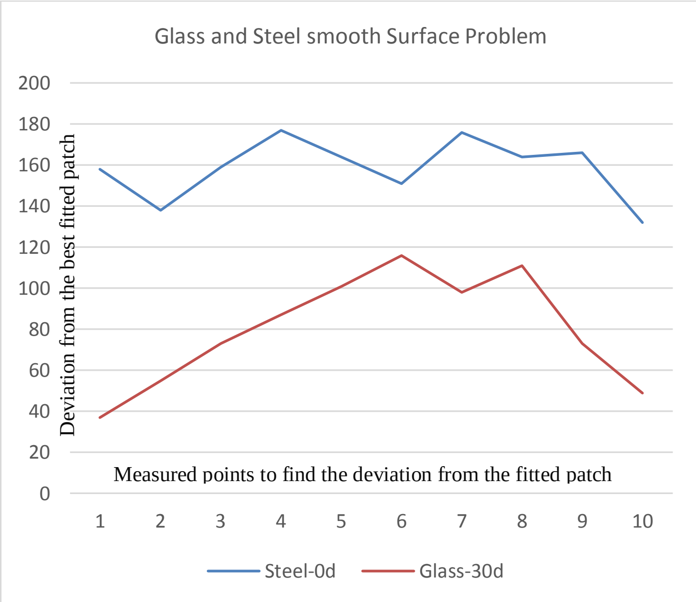

Figure 12: Deviation from the fitted patch for these points that have noise due to the Sun shine during scanning objects.

3.3 Overall RMSEs Results of Different Scanning

Figure 13 and Table 8 below shows the overall RMSEs for all selected materials. Generally, RMSEs results from the scanning of smooth surface was greater than produced from the scanning of rough surface in all condition, due to macro-facet parts on the surface of the rough surfaces. Totally, the maximum RMSE was recorded for the glass material in all three scan angles, except of the steel surface at zero degree incident angle. The reason of this huge difference that happened at zero degree on the steel surface is due to the effect of the sun shine on the material surface. In terms of painted surfaces RMSE of the black and red colours were greater than the other green, blue and white colours based on the differences of intensity value between colours. The reflectivity variation was highly appeared on the smooth surface in comparison with the rough surfaces because the rough surface reduce the effects of the scan angle and intensity values between the objects and colours in all selected scan angles.

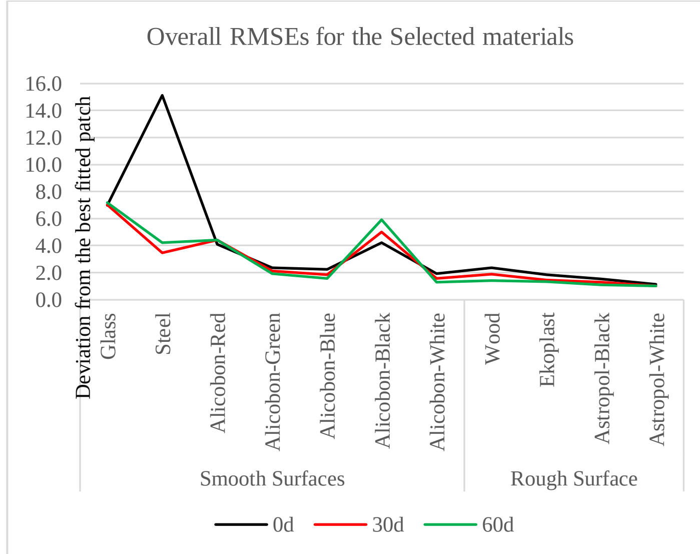

Figure 13: Overall RMSEs of the selected materials for rough and smooth surfaces at 0, 30, and 60 scan angles.

Table 8: All overall RMSE deviations from the best fitted patch for rough and smooth surfaces at 0, 30, and 60 degree scan angles.

Surface Properties	Materials	0d (mm)	30d (mm)	60d (mm)
Smooth Surfaces	Glass	7.0	7.0	7.2
	Steel	15.1	3.5	4.2
	Alicobon-Red	4.1	4.4	4.43
	Alicobon-Green	2.37	2.12	1.92
	Alicobon-Blue	2.24	1.84	1.55
	Alicobon-Black	4.2	5	5.9
	Alicobon-White	1.92	1.55	1.3
Rough Surface	Wood	2.37	1.88	1.41
	Ekoplast	1.86	1.46	1.32
	Astropol-Black	1.5	1.3	1.1
	Astropol-White	1.2	1.0	1.0

4. Conclusion

Due to high accuracy level in the measuring data, TLS is an instrument performed in most different industries that require the milli-metric accuracy level and complex objects, like monitoring, recording of extremely expensive heritage objects, and calibration of oil tanks. Nevertheless, TLS is not immune to mistakes that arise during the data capture process when scanning objects. Three primary aspects determine the accuracy of the measurement data: the scanner's ability to measure the time of flight of the laser beam, the properties of the scanned materials, and the scanner's range detector. The practical experiments conducted in this research reveals some important results regarding the Sun shine, colors, , surface qualities and incident angles all of which should be considered when aiming for extremely high TLS object scanning performance.

Firstly, materials with a rough surface have a higher reflectivity than those with a smooth surface. Because of the micro-faced parts on their surfaces, wood and ekoplast have rough surfaces and do not record high deviation values at 0˚ to 60˚ of impact angle; in contrast, steel and glass, which have smooth surfaces did record higher deviation values at 0˚ to 60˚ from rough surface materials.

Secondly, At higher incident angles, such as 60˚ or greater, the amount of signal returned from smooth surfaces may become insufficient for accurate point cloud detection. In some cases, no point clouds are measured at all, especially when the surface is exceptionally smooth or the material's reflectivity is low. Can be supported by (Amer et al., 2018) concluded that the scanning accuracy is directly decreased with the increase of used projection angle.

Thirdly, the degree of accuracy in measuring 3D data varies depending on the material due to differences in its transmission, absorption, roughness, and reflected laser signal. Because of this, the point clouds' accuracy varied depending on the type of substance.

Fourthly, the accuracy and quality of single point cloud measuring on smooth surfaces for steel and glass materials is seriously compromised if the incident angle aligns with the angle at which the Sun shines incidentally. This is because the laser beam returns to the scanner more quickly. For steel materials, this phenomena happened at a zero degree incident angle, whereas for glass materials, it happened at a 30º incident angle.

Surfaces with high reflectivity and smoothness pose specific challenges. For laser class-1 scanners, no point clouds are returned at any incident angle or range. Laser class-3 scanners may reflect the beam, but at an accelerated rate, leading to positional errors. Even with TS targets placed on these surfaces, no reflected point clouds are observed across all incident angles and ranges.

Subsequently, the total RMSE of the scanned surface as well as the quantity of returned point clouds will depend on the color intensity. The intensity of black color is smaller than the other colors because it has 5.9mm RMSE at 60˚ scan angle, while for the white color on the same surface and incident angle the RMSE is 1.3mm. The reflectivity of the returning signal rises with intensity, and the RMSE as a whole falls.

The range was affected on the accuracy of measuring point clouds in terms of quality and intensity of the returned laser beam. And periodical time for scanning the same surface of an object increases with increasing the range.

References

Abbas, M. A., Setan, H., Majid, Z., Chong, A. K., Lichti, D. D., & Idris, K. M. (2014). Improvement in accuracy through self-calibration for panoramic scanner. Lecture Notes in Geoinformation and Cartography, 0(March), 201–217. https://doi.org/10.1007/978-3-319-03644-1_15

Abbass, Z. D., Maatooq, J. S., & Al-mukhtar, M. M. (2023). Monitoring and Modelling Morphological Changes in Rivers Using RS and GIS Techniques. March. https://doi.org/10.28991/CEJ-2023-09-03-03

Abdurrahman Farsat1*, Martin J. Smith, & Nikkolas Kokkas. (2014). The importance of designing targets for improving the accuracy of Mobile Laser Scanning data. Conference 2nd -5th September at Aberstwyth University. Available at Conference Booklet, Technical Section Lidar. P.P 86-92, May.

Amer, H. A., Shaker, I. F., Abdel-gawad, A. K., Ragab, A., & Mogahed, Y. (2018). Accuracy Assessment of Laser Scanner under Different Projections Angles. 428–438.

Bae, K., & Belton, D. (2012). A Framework for Position Uncertainty of Unorganised Three-Dimensional Point Clouds from Near-Monostatic Laser Scanners Using Covariance Analysis. May.

Bae, K., & Lichti, D. D. (2007). On-site self-calibration using planar features for terrestrial laser scanners. ISPRS Workshop on Laser Scanning, 36(1), 14–19.

Balzani, V. (n.d.). Electron Transfer in Chemistry ®WILEY~VCH Weinheim • New York • Chichester Brisbane • Singapore • Toronto.

Chan, T. O., Lichti, D. D., & Belton, D. (2015a). A rigorous cylinder-based self-calibration approach for terrestrial laser scanners. ISPRS Journal of Photogrammetry and Remote Sensing, 99, 84–99. https://doi.org/10.1016/j.isprsjprs.2014.11.003

Chan, T. O., Lichti, D. D., & Belton, D. (2015b). A rigorous cylinder-based self-calibration approach for terrestrial laser scanners. ISPRS Journal of Photogrammetry and Remote Sensing, 99(June 2018), 84–99. https://doi.org/10.1016/j.isprsjprs.2014.11.003

Date, H., Wakisaka, E., Moribe, Y., Kanai, S., Vi, C., & Vi, W. G. (2019). TLS POINT CLOUD REGISTRATION BASED ON ICP ALGORITHM USING POINT QUALITY. XLII(June), 10–14.

Gordon, S., Lichti, D. D., Stewart, M. P., & Tsakiri, M. (2000). <title>Metric performance of a high-resolution laser scanner</title>. Videometrics and Optical Methods for 3D Shape Measurement, 4309(December 2000), 174–184. https://doi.org/10.1117/12.410872

Huang, X., Zhang, Y., Ni, B., Li, T., Chen, K., & Zhang, W. (2023). Boosting Point Clouds Rendering via Radiance Mapping. Proceedings of the AAAI Conference on Artificial Intelligence, 37(1), 953–961. https://doi.org/10.1609/aaai.v37i1.25175

Kostrikov, S., Pudlo, R., Bubnov, D., & Vasiliev, V. (2020). ELiT, Multifunctional Web-Software for Feature Extraction from 3D LiDAR Point Clouds. ISPRS International Journal of Geo-Information, 9(11), 650. https://doi.org/10.3390/ijgi9110650

Lichti, D. D., & Harvey, B. . (2002). the Effects of Reflecting Surface Material Properties on Time-of-Flight Laser Scanner Measurements. Geospatial Theory, Processing and Applications, 2001.

Mala, B. A., & Al-shrafany, D. M. S. (2023). The influence of the incident angles variation on the accuracy of TLS point cloud based on surface reflectivity and roughness. 2023(08), 94–112.

Mala, B. A., Salih, D. M., & Sadeq, A.-J. (2016). Integration of Terrestrial Laser Scanning and Digital Close-Range Photogrammetry for Heritage Documentation. November. https://zancojournals.su.edu.krd/index.php/JPAS

Murtiyoso, A., & Grussenmeyer, P. (2018). Comparison and assessment of 3d registration and georeferencing approaches of point clouds in the case of exterior and interior heritage building recording. International Archives of the Photogrammetry, Remote Sensing and Spatial Information Sciences - ISPRS Archives, 42(2), 745–751. https://doi.org/10.5194/isprs-archives-XLII-2-745-2018

Soudarissanane, S. (2016). The Geometry of Terrestrial Laser Scanning: Identification of Errors, Modelling and Mitigation of Scanning Geometry. https://repository.tudelft.nl/islandora/object/uuid%3Ab7ae0bd3-23b8-4a8a-9b7d-5e494ebb54e5

Soudarissanane, Sylvie, Lindenbergh, R., & Gorte, B. (2008). Reducing the error in terrestrial laser scanning by optimizing the measurement set-up. International Archives of the Photogrammetry, Remote Sensing and Spatial Information Sciences, XXXVII(B5), 615–620.

Soudarissanane, Sylvie, Lindenbergh, R., Menenti, M., & Teunissen, P. (2009). Incidence Angle Influence on the Quality of Terrestrial Laser Scanning Points. Iaprs, XXXVIII, 183–188.

Soudarissanane, Sylvie, & Ree, J. Van. (2007). Error budget of terrestrial laser scanning : influence of the incidence angle on the scan quality. May 2014. https://doi.org/10.13140/RG.2.1.1877.6404

Steinvall, O. (2007). Influence of laser radar sensor parameters on range-measurement and shape-fitting uncertainties. Optical Engineering, 46(10), 106201. https://doi.org/10.1117/1.2789654

Tan, K., Zhang, W., Shen, F., & Cheng, X. (2018). Investigation of TLS Intensity Data and Distance Measurement Errors from Target Specular Reflections. https://doi.org/10.3390/rs10071077